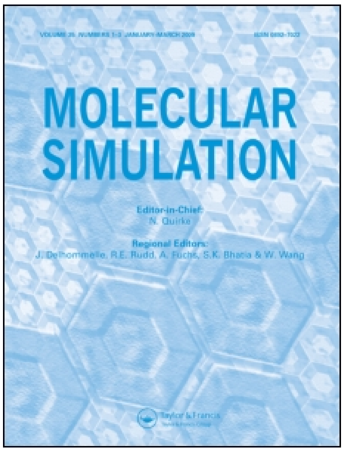

Molecular Simulation
Publication details, including instructions for authors and subscription information:
http://www.informaworld.com/smpp/title~content=t713644482

Theoretical Study of the Monomer Reaction Mechanism on Phillips CrO_x/SiO_2 Catalyst Using Density Functional Theory (DFT) and Paired Interacting Orbitals (PIO) Methods

Boping Liu[a]; Yuwei Fang[a]; Minoru Terano[a]
[a] School of Materials Science, Japan Advanced Institute of Science and Technology, Ishikawa, Japan

To cite this Article Liu, Boping , Fang, Yuwei and Terano, Minoru(2004) 'Theoretical Study of the Monomer Reaction Mechanism on Phillips CrO_x/SiO_2 Catalyst Using Density Functional Theory (DFT) and Paired Interacting Orbitals (PIO) Methods', Molecular Simulation, 30: 13, 963 — 971

To link to this Article: DOI: 10.1080/08927020412331298711

URL: http://dx.doi.org/10.1080/08927020412331298711

Molecular Simulation, Vol. 30 (13–15), 15 November–30 December 2004, pp. 963–971

Taylor & Francis
Taylor & Francis Group

Theoretical Study of the Monomer Reaction Mechanism on Phillips CrO_x/SiO_2 Catalyst Using Density Functional Theory (DFT) and Paired Interacting Orbitals (PIO) Methods

BOPING LIU, YUWEI FANG and MINORU TERANO*

School of Materials Science, Japan Advanced Institute of Science and Technology, 1-1 Asahidai, Tatsunokuchi, Ishikawa 923-1292, Japan

(Received January 2004; In final form January 2004)

The importance of Phillips CrO_x/SiO_2 catalyst could still be reflected from its 7 million tons of world HDPE production. However, the activation mechanism of this catalyst by ethylene in terms of active sites formation still remains unclear. In this work, the paired interacting orbital (PIO) method combined with density functional theory (DFT) calculation was applied for the theoretical studies on the intermolecular orbital interactions between ethylene monomer and a molecular model of surface monochromate species under six typical intermolecular geometric orientations (GO-1 ~ GO-6). Both DFT and PIO results indicated that GO-2 orientation should be the most preferential orientation for the reaction between ethylene monomer and monochromate species. Within GO-2 orientation the ethylene monomer preferentially approaches to the surface monochromate Cr(VI) species in a symmetric orientation relative to the two carbon atoms of ethylene from the upper site between the two double-bonded oxo-atoms of surface monochromate species. The electronic and orbital origin of the GO-2 orientation was elucidated in terms of its low energy increase due to lower repulsive interaction and in-phase overlap of molecular orbital interaction in-between the intermolecular frontier region.

Keywords: Phillips CrO_x/SiO_2 catalyst; Monochromate site; Ethylene; Chromic acid; Density functional theory (DFT); Paired interacting orbitals (PIO)

INTRODUCTION

As one of the most important industrial olefin polymerization catalysts, Phillips CrO_x/SiO_2 catalyst is still attracting both academic and industrial interest [1–7]. Compared with Ziegler-Natta and metallocene catalysts, Phillips catalyst has quite unique and competitive characteristics, especially for the capability to produce high density polyethylene (HDPE) featured with ultra-broad molecular weight distribution and long chain branching [8]. The polymer usually shows ideal processibility especially for blow molding [8,9]. These unique polymer structures and properties were supposed to originate from its most significantly interesting polymerization behavior that it shows high polymerization activity without using any activator like alkyl-aluminum or MAO [9]. Ethylene can act as an activator to reduce the hexavalent chromate species ($Cr(VI)O_{x,surf}$) into surface-stabilized divalent chromium species ($Cr(II)O_{x,surf}$) followed by alkylation of the $Cr(II)O_{x,surf}$ before the initiation of ethylene polymerization [6,7,9]. In fact, the specific mechanisms concerning the activation including reduction and alkylation of surface $Cr(VI)O_{x,surf}$, still remains mysterious even after 50 years of great research efforts [9,10]. This study will focus on the mechanism relating to the reduction of $Cr(VI)O_{x,surf}$ to $Cr(II)O_{x,surf}$ by ethylene, which is corresponding to the first step in activation of Phillips catalyst.

The $Cr(VI)O_{x,surf}$ on calcined Phillips catalyst may exist as monochromate, dichromate and sometimes even polychromate species (for plausible structures, please see Fig. 2 in Ref. [5]). Our recent experimental studies on the induction period of ethylene polymerization using the Phillips catalyst have shown that the ethylene monomer first reduces the $Cr(VI)O_{x,surf}$ to $Cr(II)O_{x,surf}$ with the simultaneous formation of two formaldehyde molecules [6,7]. According to the mechanism based on this experimental evidence, the ethylene monomer must approach the surface $Cr(VI)O_{x,surf}$ in a symmetric orientation relative to the two carbon atoms of

---

*Corresponding author. Tel.: +81-761-51-1620. Fax: +81-761-51-1625. E-mail: terano@jaist.ac.jp

ISSN 0892-7022 print/ISSN 1029-0435 online © 2004 Taylor & Francis Ltd
DOI: 10.1080/08927020412331298711

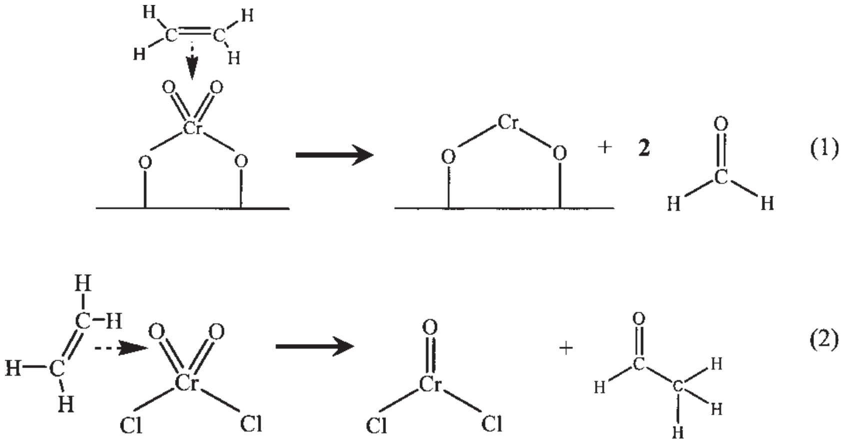

SCHEME 1 Proposed mechanisms of the reduction of hexavalent Cr compounds by ethylene determined by preferential molecular orientation between the two reacting molecules resulting in completely different reaction products.

ethylene and the two double-bonded oxo-atoms from the upper site (see reaction (1) in Scheme 1 using monochromate species as an example) [6]. The origin of this most preferential geometric orientation between ethylene molecule and the monochromate species is still unclear. In the literature, Limberg *et al.* proposed a completely different reduction route of hexavalent chromyl chloride by ethylene due to different molecular orientation between the hexavalent Cr species and ethylene molecule (see reaction (2) in Scheme 1) [11]. According to their speculation, the ethylene approaches to chromyl chloride from the side direction between the oxygen and chlorine atoms rather than from the upper side between the two double-bonded oxo-atoms leading to the formation of a tetravalent Cr species and acetaldehyde as final products [11]. The molecular orbital interactions between hexavalent Cr species and ethylene molecule could be considered as the driving force behind these most interesting intermolecular orientation-directed reactions, which has never been studied before. In this work, the molecular orbital interactions under various intermolecular geometric orientations between ethylene monomer and surface monochromate species will be studied through a theoretical approach in combination of density functional theory (DFT) and molecular orbitals (MO) calculation methods.

In recent decades, there has been an academic booming in the theoretical studies on heterogeneous olefin polymerization catalysts using various computation methods including DFT and MO [2,3,12–15], though the majority of these studies are almost exclusively focused on Ziegler-Natta catalysts. Systematic theoretical research on the Phillips catalyst is crucial for further development in the field of olefin polymerization catalysts and Cr-related chemistry [2,3]. For the purpose of the study on intermolecular orbital interaction between ethylene monomers and surface monochromate species, the paired interacting orbitals (PIO) method, which was developed by Fujimoto *et al.* [16] based on the frontier orbital theory of Fukui [17], seemed to be the most powerful one among various MO methods. DFT method would be utilized to facilitate the PIO analysis through obtaining the optimized geometric structures of the interacting molecular compounds as well as their electronic properties. The PIO method described the intermolecular interaction based on multi-orbitals interaction including not only the frontier orbitals, which include the highest occupied molecular orbital (HOMO) and the lowest unoccupied molecular orbitals (LUMO), but also other molecular orbitals. It has been proven to be mostly useful for the studies on transition metal-contained complex system [14,15,18]. This method has been applied only for the theoretical study on Ziegler-Natta catalysts by Shiga *et al.* [18,19]. PIO method combined with DFT calculation was applied in this paper for the theoretical study on the molecular orbital interactions between ethylene monomer and a molecular model of surface monochromate species under various intermolecular geometric orientations. As for the model compound of the monochromate species on Phillips catalyst, chromic acid was taken as a simple model for this preliminary PIO calculation (see Fig. l). The calculated results were expected not to be significantly affected by

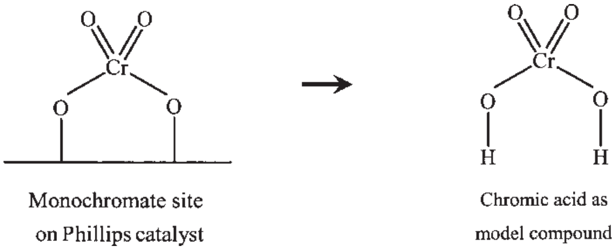

FIGURE 1 Chromic acid as molecular model for monochromate site on industrial calcined Phillips CrO_x/SiO_2 catalyst.

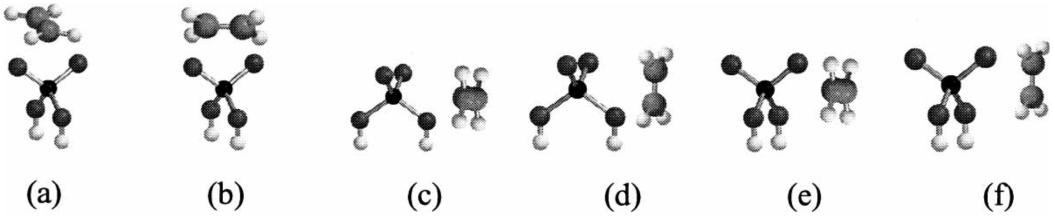

FIGURE 2 Six typical molecular orientations between chromic acid and ethylene considered for the calculation of molecular orbital interaction by PIO method in this work, (a) GO-1; (b) GO-2; (c) GO-3; (d) GO-4; (e) GO-5 and (f) GO-6. The elements are coded in an increasing gray scale sequence as follows: H (white) < C < O < Cr (black).

using chromic acid as model compound thinking of its less steric effect from the two hydrogen atoms to the up-coming ethylene molecule compared with the surface of silica gel. The calculated results shown in this work have demonstrated that a theoretical understanding of the driving force for the intermolecular orientation-directed reaction between monochromate site and ethylene has been obtained in a molecular orbital level.

COMPUTATIONAL METHODS

The details concerning the basic theoretic and mathematic bases of PIO method can be found in the literature and will not be introduced again herein [18,20]. The equilibrium structure of ethylene monomer and molecular model of monochromate species (chromic acid) in ground state were calculated by DFT method (RB3LYP, basis set: 6-31G**) using SPARTAN'02 Windows developed by Wavefunction, Inc. The surface electron density, surface potential, dipole and electrostatic charge of each atom in both molecules were obtained. These optimized molecular structures were used for the subsequent PIO calculations. LUMMOX software for Windows PC computer, which was developed by Sumitomo Chem. Corp. based on the PIO theory established by Fujimoto *et al.* [16,20], was used for calculation of intermolecular orbital interaction by PIO method. As shown in Fig. 2, six typical intermolecular orientations namely GO-1, GO-2, GO-3, GO-4, GO-5 and GO-6 between chromic acid and ethylene with an intermolecular distance of 3 Å (distance between Cr atom and C=C bond) were calculated by PIO method. The interacting molecular system between chromic acid and ethylene was defined as combined system C, in which chromic acid molecule and ethylene molecule were named as fragments A and B. The extended Hüeckel calculations were used to obtain the canonical molecular orbitals. The interaction between A and B in C could be well represented by 12 pairs of localized orbitals. In each orbital pair, one orbital belongs to fragment A and the other to fragment B. Based on these calculation results from both DFT and PIO methods, the most preferential geometric orientation between molecules A and B was achieved, which was inconsistent with conventional mechanism speculated from experimental evidence. Moreover, electronic and molecular orbital origins behind the intermolecular orientation-directed reaction between chromate species and ethylene in the activation of Phillips catalyst for ethylene polymerization have been elucidated.

RESULTS AND DISCUSSION

The optimized equilibrium geometry structures of both the chromic acid and ethylene molecules were calculated using the DFT RB3LYP method with a 6-31G** basis set. The equilibrium structure parameters of chromic acid are shown in Table I including a comparison with reference data reported by Johnson and Panas [21]. As can be seen from Table I, the structural data including bond lengths and bond angles for chromic acid equilibrium ground state are almost the same as those reported in the literature. Only the Cr—O—H angle of 122.8° is slightly lower compared with 137.5°. This deviation did not affect our calculation results, which was confirmed by calculation using the reference structural data and will be discussed in the later section. The electron density, dipolar property, molecular orbitals of HOMO and LUMO of chromic acid computed by DFT method are all shown in Fig. 3. The dipolar property of chromic acid shows a value of 4.48 debye with the positive cationic center in-between the two hydrogen atoms and the negative anionic center around the Cr atom.

TABLE I Equilibrium geometry of chromic acid calculated by DFT method and a comparison with reference data in the literature

Geometry parameters of chromic acid		*This work**	*Reference data [21]*
Bond lengths (Å)	Cr=O	1.562	1.567
	Cr—O	1.754	1.729
	O—H	0.966	0.967
Bond angles (°)	O=Cr=O	107.83	107.4
	O=Cr—O	109.60	110.2
	O—Cr—O	110.57	108.7
	Cr—O—H	122.80	137.5

*Computation conditions: DFT method RB3LYP, basis set: 6-31G**, number of shells: 29, number of basic functions: 99.

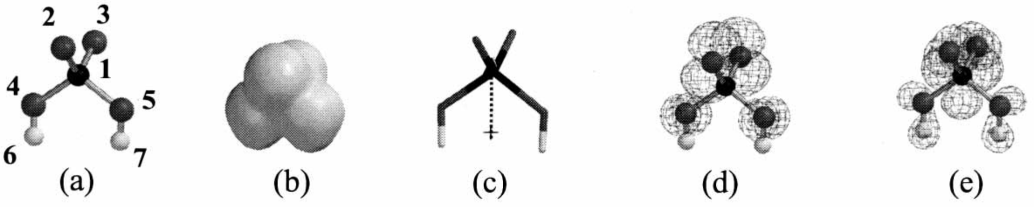

FIGURE 3 Electron density, electrostatic potential, molecular orbitals of HOMO and LUMO of chromic acid computed by DFT method, (a) equilibrium geometry; (b) electron density; (c) dipole; (d) HOMO and (e) LUMO.

The HOMO of chromic acid mostly comprised of atomic orbitals from the oxygen atoms ((O(2), O(3), O(4) and O(5)). Moreover, it can be clearly observed that the contribution from the upper two double-bonded oxo-atoms (O(2) and O(3)) in the HOMO is obviously larger than that from the two oxygen atoms on the left and right sides (O(4) and O(5)). The LUMO of chromic acid comprised of a large contribution from atomic orbitals of Cr(1) atom and a small fraction from the oxygen and hydrogen atoms (O(4), O(5), H(6) and H(7)). The energy of the HOMO and LUMO of chromic acid is -8.66 and -4.52 eV, respectively, with a band gap of 4.14 eV. The most interesting and important results from the DFT calculation is the electrostatic potential of the chromic acid model, and the atomic charges for all atoms are Cr(1): $+0.8868$, O(2) or O(3): -0.2643, O(4) or O(5): -0.5977, H(6) or H(7): $+0.4186$ with a total charge of 0. The negative charge at atom O(4) or O(5) is almost two times of that at atom O(2) or O(3). The much stronger coulombic repulsive interaction from the two atoms O(4) or O(5) to the π electrons (HOMO) might play an important role in the preferential orientation of the ethylene molecule in approaching the upper two atoms O(2) or O(3) with much lower negative charges. The equilibrium structure, electron density, dipolar property, electrostatic potential, molecular orbitals of HOMO and LUMO of ethylene monomer in ground state were also computed by DFT method with most of results shown in Fig. 4. The HOMO and LUMO of ethylene are the well-known π (bonding) and π^* (anti-bonding). The energy of the HOMO and LUMO of ethylene is -7.28 and 0.47 eV, respectively, with a band gap of 7.75 eV. The band gap between HOMO and LUMO is much larger for ethylene compared with that of chromic acid. The electrostatic potential with the atomic charges for all atoms in the ethylene monomer are C(8) or C(9): -0.2787; H(10), H(11), H(12) or H(13): $+0.1393$ with a total charge of 0. The equilibrium geometry of ethylene is shown with bond lengths (R) : $R(C{=}C) = 1.330\,Å$ and $R(C{-}H) = 1.087\,Å$, and bond angles (Δ) : $\Delta(C{=}C{-}H) = 121.83°$ and $\Delta(H{-}C{-}H) = 116.35°$. These structural parameters showed negligible deviation from literature report [13,18,19]. Due to the planar and symmetric distribution of negative (at carbon atoms) and positive (at hydrogen atoms) charges, it is reasonable to get no dipolar effect in ethylene molecule. In the following sections, those parameters of optimized molecular structures in ground state were utilized in the subsequent PIO calculations for further elucidation of the intermolecular interaction between chromic acid model and ethylene in terms of intermolecular orbital origin of the most preferential intermolecular configuration orientation.

According to the mechanism proposed previously, based on our experimental results concerning the reduction of monochromate species by ethylene in the first stage of activation of Phillips CrO_x/SiO_2 catalyst as depicted in Scheme 2 [6], the monochromate Cr(VI) species was coordinated by ethylene at the most preferential intermolecular orientation corresponding to GO-2 in Fig. 2. Subsequently, the monochromate Cr(VI) species was reduced to $Cr(II)O_{x,surf}$ through an intermediate Cr(IV) species with the simultaneous formation of two formaldehyde molecules. Consequently, it could be expected that intermolecular orbital interaction

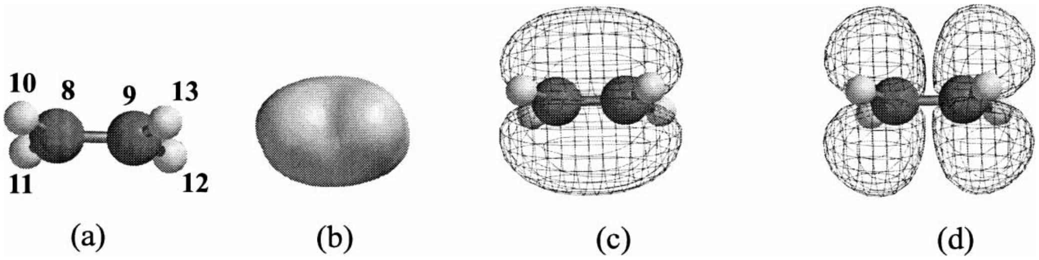

FIGURE 4 Electron density, electrostatic potential, dipolar property, molecular orbitals of HOMO and LUMO of ethylene molecule computed by DFT method, (a) equilibrium geometry; (b) electron density; (c) HOMO and (d) LUMO.

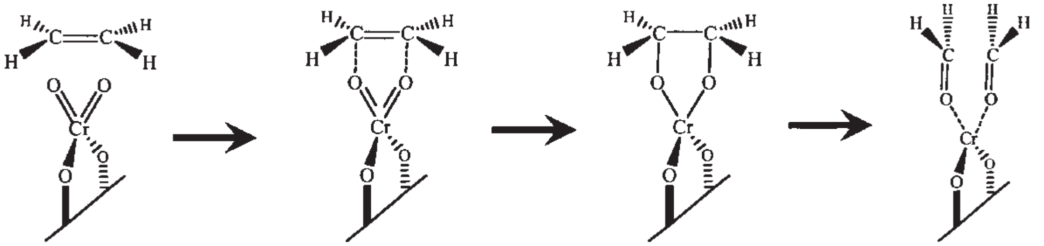

SCHEME 2 Plausible monomer reaction mechanism between ethylene and monochromate site on Phillips CrO_x/SiO_2 catalyst during the induction period of ethylene polymerization proposed based on experimental work.

using PIO method should give theoretical evidence especially in-between the intermolecular frontier area either in favor of or contrary to the potential electron delocalization for the formation of the new bonding of the intermediate in the proposed mechanism solely based on experimental evidence.

The Hückel energies of the combined interacting systems C (E_C) at an intermolecular distance of 3 Å (distance between Cr atom and C=C bond) between A (chromic acid) and B (ethylene) for the six typical intermolecular orientations namely GO-1, GO-2, GO-3, GO-4, GO-5 and GO-6, as well as the Hückel energies for isolated A ($E°_A$) and isolated B ($E°_B$), energy increase ($\Delta E_C = E_C - E°_C$, in which $E°_C = E°_A + E°_B$) before and after interaction are shown in Table II. The intermolecular distance of 3 Å was selected according to the literature [18]. Too small intermolecular distance must be avoided in order to omit the calculation deviation from the internucleic interaction, meanwhile, effective information could not be obtained if the intermolecular distance is too far away. As it can be seen from Table II, the combined interacting system C shows much lower energy increase at GO-1 and GO-2 compared with those at other four intermolecular orientations indicative of much lower repulsive interaction from the two double-bonded oxo-atoms. These results are in consistent with the DFT calculation results regarding the electrostatic charge distribution in the chromic acid model. The much weaker coulombic repulsive interaction towards the two negatively charged carbon atoms in ethylene from the two double-bonded oxo-atoms (with almost half of the negative charges relative to the other two single-bonded oxygen atoms) should be the governing factor to direct the ethylene molecule in approaching to chromic acid from the upper two double-bonded oxo-atoms. However, the ethylene molecule is approaching in this way in both GO-1 and GO-2 with the only difference in either parallel or perpendicular to line across the two oxo-atoms O(2) and O(3). It would be still difficult and too early to judge which is more favorable between GO-1 and GO-2, before a PIO analysis of these two intermolecular orientations. The PIO orbitals for the combined interacting system C may provide crucial information regarding favorable or unfavorable electron delocalization in-between the frontier area.

TABLE II Hüeckel energies of the interacting systems under the six typical molecular orientations between chromic acid and ethylene calculated by PIO method

*Molecular orientataions**	*E_c (eV)†*	*ΔE_c (eV)‡*
GO-1	−850.41	+1.09
GO-2	−849.78	+1.72
GO-3	−847.40	+4.09
GO-4	−847.32	+4.17
GO-5	−848.69	+2.80
GO-6	−848.50	+2.99

* Intermolecular distance between Cr atom and C=C bond is 3 Å for all six orientations. † $E°_C = -851.49$ eV, C: interacting system between A and B, E_C: Hüeckel energy of interacting system C at an inter-molecular distance 3° between A and B. ‡ $\Delta E_C = E_C - E°_C$, $E°_C = E°_A + E°_B$, $E°_C$: Hüeckel energy of a summary of A and B, $E°_A$(A : chromic acid) = −637.10 eV, $E°_B$(B : ethylene) = −214.39 eV.

The extended Hüeckel calculations were used to obtain the canonical molecular orbitals for the combined interacting system C at GO-1. Twelve pairs of localized orbitals were obtained. In each orbital pair, one orbital belongs to fragment A and the other to fragment B. The eigenvalues on pairwise transformation indicate that two pairs of PIO orbitals namely PIO-1 and PIO-2 within the 12 pairs made 78.2 and 11.4% of contribution, respectively, in the intermolecular orbital interaction at GO-1 [18]. The analysis of the other 10 pairs of PIO orbitals (from PIO-3 to PIO-12) could be neglected due to their too low contribution in the interaction. The contour maps of PIO-1 and PIO-2 of the interacting system C at the intermolecular orientation GO-1 are shown in Fig. 5. Both PIO-1 and PIO-2 show out-of-phase molecular orbital interaction at GO-1, which is consistent with their negative overlap populations. These PIO molecular orbital evidences demonstrated that no favorable electronic delocalization in-between the intermolecular frontier area could be observed at GO-1 although it shows the lowest repulsive interaction. The PIO calculation results for the expression of PIO-1 and PIO-2 in terms of a linear

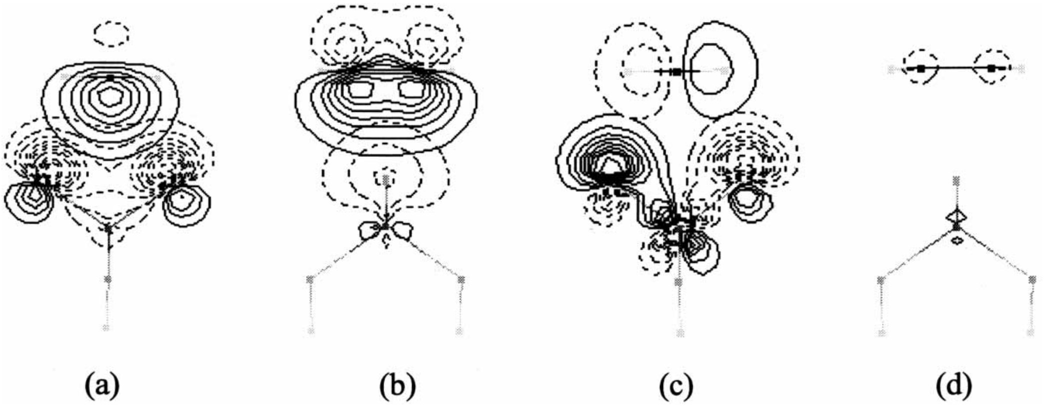

FIGURE 5 Contour maps of PIO orbitals of the interacting system C at molecular orientation GO-1, (a) PIO-1(1), (b) PIO-1(2) the cross section perpendicular to that in (a); (c) PIO-2(1), (d) PIO-2(2) the cross section perpendicular to that in (c).

combination of atomic orbitals (LCAO) are shown in Eqs. (1)–(4) as follows.

$$\begin{aligned}\text{PIO-1(A)} = {} & -0.434\text{O}(2)_{2\text{Py}} - 0.434\text{O}(3)_{2\text{Py}} \\ & - 0.310\text{Cr}(1)_{4\text{Py}} - 0.249\text{Cr}(1)_{4\text{S}} \\ & - 0.242\text{O}(2)_{2\text{S}} - 0.242\text{O}(3)_{2\text{S}} \\ & + 0.207\text{O}(2)_{2\text{Px}} - 0.207\text{O}(3)_{2\text{Px}} \\ & + 0.116\text{Cr}(1)_{3\text{Dz}^2} \ldots \end{aligned} \quad (1)$$

$$\begin{aligned}\text{PIO-1(B)} = {} & -0.494\text{C}(8)_{2\text{Py}} - 0.494\text{C}(9)_{2\text{Py}} \\ & + 0.191\text{C}(8)_{2\text{S}} + 0.191\text{C}(9)_{2\text{S}} \\ & + 0.138\text{C}(8)_{2\text{Pz}} - 0.138\text{C}(9)_{2\text{Pz}} \ldots \end{aligned} \quad (2)$$

$$\begin{aligned}\text{PIO-2(A)} = {} & -0.531\text{O}(2)_{2\text{Py}} + 0.531\text{O}(3)_{2\text{Py}} \\ & - 0.436\text{Cr}(1)_{3\text{Dxy}} - 0.317\text{Cr}(1)_{4\text{Px}} \\ & - 0.222\text{O}(2)_{2\text{S}} + 0.222\text{O}(3)_{2\text{S}} \ldots \end{aligned} \quad (3)$$

$$\begin{aligned}\text{PIO-2(B)} = {} & 0.331\text{C}(8)_{2\text{Px}} + 0.331\text{C}(9)_{2\text{Px}} \\ & - 0.305\text{H}(10)_{1\text{S}} - 0.305\text{H}(13)_{1\text{S}} \\ & + 0.305\text{H}(11)_{1\text{S}} + 0.305\text{H}(12)_{1\text{S}} \end{aligned} \quad (4)$$

Some minor contributions from various atomic orbitals were omitted in these equations, from which the main components ($\text{O}(2, 3)_{2\text{Py}}$, $\text{C}(8, 9)_{2\text{Py}}$ and $\text{C}(8, 9)_{2\text{Px}}$) of atomic orbitals can be observed to form the unfavorable repulsive interaction between A and B at GO-1. The PIO-1 and PIO-2 orbitals could also be expressed in terms of a linear combination of molecular orbitals (LCMO) calculated from molecules A and B, respectively, as shown in Eqs. (5)–(8) as follows.

$$\begin{aligned}\text{PIO-1(A)} = {} & -0.698 \ \ \text{HOMO}(-9)_\text{A} \\ & - 0.54 \ \text{HOMO}(-13)_\text{A} \\ & + 0.34 \ \text{HOMO}(-15)_\text{A} \\ & - 0.203 \ \text{LUMO}(+9)_\text{A} \\ & - 0.116 \ \text{LUMO}_\text{A} \ldots \end{aligned} \quad (5)$$

$$\begin{aligned}\text{PIO-1(B)} = {} & -0.789 \ \text{HOMO}_\text{B} + 0.595 \ \text{HOMO}(-5)_\text{B} \\ & - 0.135 \ \text{LUMO}(+4)_\text{B} \\ & - 0.077 \ \text{HOMO}(-1)_\text{B} \end{aligned} \quad (6)$$

$$\begin{aligned}\text{PIO-2(A)} = {} & 0.684 \ \text{HOMO}(-12)_\text{A} + 0.487 \ \text{HOMO}_\text{A} \\ & - 0.398 \ \text{HOMO}(-3)_\text{A} \\ & + 0.269 \ \text{LUMO}(+10)_\text{A} \ldots \end{aligned} \quad (7)$$

$$\begin{aligned}\text{PIO-2(B)} = {} & 0.999 \ \text{HOMO}(-3)_\text{B} \\ & + 0.048 \ \text{LUMO}(+1)_\text{B} \end{aligned} \quad (8)$$

For molecule A (chromic acid), the molecular orbital calculation was performed with a total electron number of 32 and a total MO number of 27. The 16 occupied MOs in a deceasing sequence in energy are named as HOMO_A, $\text{HOMO}(-1)_\text{A}$, $\text{HOMO}(-2)_\text{A}$, …, $\text{HOMO}(-15)_\text{A}$, respectively. The 11 unoccupied MOs in increasing sequence in energy are named as LUMO_A, $\text{LUMO}(+1)_\text{A}$, $\text{LUMO}(+2)_\text{A}$, …, $\text{LUMO}(+10)_\text{A}$, respectively. As for molecule B (ethylene), the molecular orbital calculation was performed with total electron number of 12 and total MO number of 12. Similarly, the six occupied MOs and six unoccupied MOs are defined as HOMO_B, $\text{HOMO}(-1)_\text{B}$, $\text{HOMO}(-2)_\text{B}$, …, $\text{HOMO}(-5)_\text{B}$ and LUMO_B, $\text{LUMO}(+1)_\text{B}$, $\text{LUMO}(+2)_\text{B}$, …, $\text{LUMO}(+5)_\text{B}$, respectively. In Eqs. (5)–(8), those minor contributions from various molecular orbitals were omitted. The main components of molecular orbitals for PIO orbitals of GO-1 for the formation of the unfavorable repulsive interaction between A and B at GO-1 can be observed to be $\text{HOMO}(-9)_\text{A}$, $\text{HOMO}(-13)_\text{A}$, HOMO_B, $\text{HOMO}(-5)_\text{B}$ for PIO-1 and $\text{HOMO}(-12)_\text{A}$, $\text{HOMO}(-3)_\text{B}$ for PIO-2, respectively. It is noticeable that the intermolecular orbital interactions at GO-1 are mostly derived from occupied MOs from both A and B.

The extended Hüeckel calculations were also used to obtain the canonical molecular orbitals for

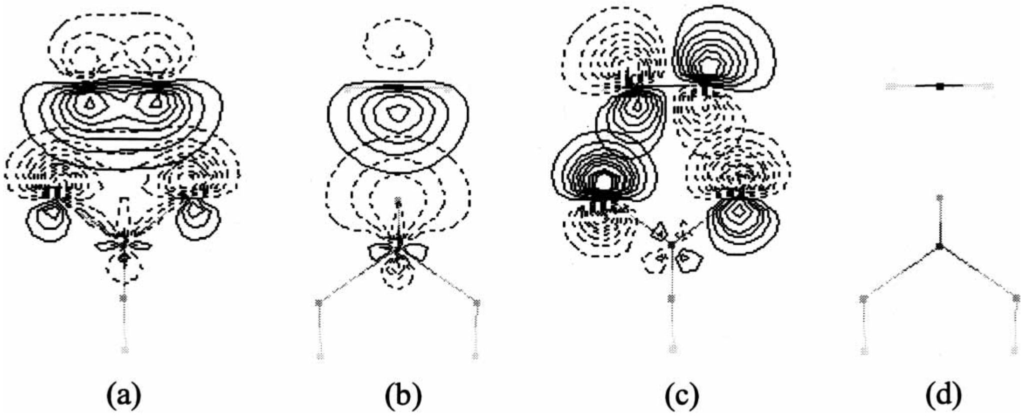

FIGURE 6 Contour maps of PIO orbitals of the interacting system C at molecular orientation GO-2, (a) PIO-1(1), (b) PIO-1(2) the cross section perpendicular to that in (a); (c) PIO-2(1), (d) PIO-2(2) the cross section perpendicular to that in (c).

the combined interacting system C at GO-2. Twelve pairs of localized orbitals were obtained. In each orbital pair, one orbital belongs to fragment A and the other to fragment B. The eigenvalues on pairwise transformation indicate that two pairs of PIO orbitals namely PIO-1 and PIO-2 within the 12 pairs made 63.9 and 28.2% of contribution, respectively, in the intermolecular orbital interaction at GO-2 [18]. Further PIO analysis will focus solely on PIO-1 and PIO-2 orbitals due to too low contribution from the other 10 PIO orbitals in the interaction. The contour maps of PIO-1 and PIO-2 of the interacting system C at the intermolecular orientation GO-2 are shown in Fig. 6. PIO-1 still shows out-of-phase molecular orbital interaction at GO-2, which is consistent with their negative overlap populations. However, PIO-2 shows in-phase molecular orbital interaction indicating favorable electron delocalization at GO-2. Moreover, PIO-2 shows a positive electron overlap population. These PIO molecular orbital evidences demonstrated that there exists favorable electronic delocalization in-between the intermolecular frontier area that could be observed at GO-2. Furthermore, the delocalized electrons are situated at the intermolecular frontier area just in-between the carbon atoms of ethylene and the double-bonded oxygen atoms in chromic acid, where electron delocalization should favor the forthcoming formation of new bonding in the intermediate as shown in Scheme 2 [14,15,19]. The PIO calculation results of GO-2 for the expressions of PIO-1 and PIO-2 in terms of LCAO and LCMO are shown in Eqs. (9)–(12) and Eqs. (13)–(16), respectively, neglecting those minor contributions.

$$\begin{aligned}\text{PIO-1(A)} = {} & -0.414\text{O}(2)_{2\text{Py}} - 0.414\text{O}(3)_{2\text{Py}} \\ & - 0.370\text{Cr}(1)_{4\text{Py}} - 0.297\text{Cr}(1)_{4\text{S}} \\ & - 0.242\text{O}(2)_{2\text{S}} - 0.242\text{O}(3)_{2\text{S}} \\ & + 0.185\text{Cr}(1)_{3\text{Dx}^2-\text{y}^2}\ldots \end{aligned} \tag{9}$$

$$\begin{aligned}\text{PIO-1(B)} = {} & -0.5\text{C}(8)_{2\text{Py}} - 0.5\text{C}(9)_{2\text{Py}} \\ & + 0.14\text{C}(8)_{2\text{S}} + 0.14\text{C}(9)_{2\text{S}}\ldots \end{aligned} \tag{10}$$

$$\begin{aligned}\text{PIO-2(A)} = {} & -0.673\text{O}(2)_{2\text{Py}} + 0.673\text{O}(3)_{2\text{Py}} \\ & - 0.190\text{O}(2)_{2\text{S}} + 0.190\text{O}(3)_{2\text{S}} \\ & - 0.135\text{Cr}(1)_{3\text{Dxy}}\ldots \end{aligned} \tag{11}$$

$$\begin{aligned}\text{PIO-2(B)} = {} & 0.694\text{C}(8)_{2\text{Py}} - 0.694\text{C}(9)_{2\text{Py}} \\ & + 0.129\text{C}(8)_{2\text{Px}} + 0.129\text{C}(9)_{2\text{Px}}\ldots \end{aligned} \tag{12}$$

$$\begin{aligned}\text{PIO-1(A)} = {} & -0.663\,\text{HOMO}(-9)_\text{A} \\ & -0.566\,\text{HOMO}(-13)_\text{A} \\ & +0.344\,\text{HOMO}(-15)_\text{A} \\ & -0.239\,\text{LUMO}(+9)_\text{A} \\ & -0.238\,\text{HOMO}(-5)_\text{A}\ldots \end{aligned} \tag{13}$$

$$\begin{aligned}\text{PIO-1(B)} = {} & -0.798\,\text{HOMO}_\text{B} + 0.564\,\text{HOMO}(-5)_\text{B} \\ & -0.163\,\text{LUMO}(+4)_\text{B} \\ & -0.138\,\text{HOMO}(-1)_\text{B} \end{aligned} \tag{14}$$

$$\begin{aligned}\text{PIO-2(A)} = {} & -0.645\,\text{HOMO}(-3)_\text{A} + 0.64\,\text{HOMO}_\text{A} \\ & +0.359\,\text{HOMO}(-12)_\text{A} \\ & -0.198\,\text{HOMO}(-6)_\text{A}\ldots \end{aligned} \tag{15}$$

$$\begin{aligned}\text{PIO-2(B)} = {} & 0.836\,\text{LUMO}_\text{B} - 0.529\,\text{HOMO}(-4)_\text{B} \\ & +0.12\,\text{LUMO}(+5)_\text{B} \\ & -0.077\,\text{LUMO}(+2)_\text{B} \end{aligned} \tag{16}$$

The main components of atomic orbitals for PIO-1 at GO-2 can be observed to be $\text{O}(2, 3)_{2\text{Py}}$ and $\text{C}(8, 9)_{2\text{Py}}$ AOs corresponding to $\text{HOMO}(-9)_\text{A}$ $\text{HOMO}(-13)_\text{A}$ HOMO_B $\text{HOMO}(-5)_\text{B}$ MOs, which are mainly occupied orbitals from both A and B indicative of unfavorable repulsive intermolecular interaction. However, as for PIO-2, the situation seems completely different. The main orbital components for PIO-2 at GO-2 composed of $O(2,3)_{2Py}$ and $C(8, 9)_{2Py}$ AOs corresponding to $HOMO(-3)_A$, $HOMO_A$, $LUMO_B$ MOs, which are mainly intermolecular orbital interaction between the occupied orbitals from A (containing a large contribution from $HOMO_A$) and the unoccupied orbitals from B (mostly from $LUMO_B$) indicative of favorable extractive intermolecular interaction. In particular, such electron delocalization from PIO-2 at GO-2 not only favors the new bonding formation in-between the carbon atoms C(8) and O(2) or C(9) and O(3), but also assists the partial splitting of the C═C bond due to the anti-bonding feature of the $LUMO_B$ [18]. It was further confirmed that no PIO orbitals at GO-3, GO-4, GO-5 and GO-6 show such favorable extractive intermolecular interaction between A and B. In summary, the orbital interaction in terms of PIO-2 at GO-2 might be the initial driving force for the reduction of monochromate species by ethylene. The repulsive interaction from the PIO-1 might push the gradual opening of the O═Cr═O bond angle, and this might in return decrease the repulsion force and promote further reaction between the two molecules [14,18,19]. Further calculations concerning the specific energy barriers for the reactions shown in Scheme 2 and using better model compound of the silica surface are still in progress.

CONCLUSIONS

It has been demonstrated that a theoretical understanding of the driving force for the preferential intermolecular orientation between a model of monochromate site and ethylene mimicking the first stage of activation reaction of Phillips catalyst has been obtained through the combination of PIO method with DFT calculations. Firstly, the DFT calculation indicated that much stronger coulombic repulsive interaction from two single-bonded oxygen atoms O(4) or O(5) to the π electrons (HOMO) of ethylene might play the most important role in the preferential orientation of ethylene in approaching the two upper double-bonded oxo-atoms O(2) or O(3) with much lower negative charges. This was further confirmed by PIO calculations based on the optimized equilibrium structures from DFT method. The much lower intermolecular repulsive interaction in terms of much lower energy increase at GO-1 and GO-2 orientations is consistent with the electrostatic potential distribution. Further PIO analysis of intermolecular orbital interaction at GO-1 and GO-2 in terms of LCAO and LCMO expressions elucidated the atomic and molecular orbital origins of the interactions and illustrated that only PIO-2 at GO-2 shows favorable extractive intermolecular interaction between A and B with respect to electron delocalization in-between the intermolecular frontier region. Such electron delocalization, which may not only favor the new bonding formation but also assist the partial splitting of the C═C bond, might be one of the driving forces in the early stage of reduction of monochromate site by ethylene on Phillips catalyst as implied from experimental work.

Acknowledgements

The authors are grateful to Dr Akinobu Shiga, LUMMOX Research Laboratory, Japan for his valuable advices and kind help for this work.

References

[1] Gaspar, A.B., Brito, J.L.F. and Dieguez, L.C. (2003) "Characterization of chromium species in catalysts for dehydrogenation and polymerization", *J. Mol. Catal. A: Chem.* **203**, 251.

[2] Schmid, R. and Ziegler, T. (2000) "Ethylene-polymerization by surface supported Cr(IV) species: possible reaction mechanisms revisited by theoretical calculations", *Can. J. Chem.* **78**, 265.

[3] Espelid, Ø. and Børve, K.J. (2002) "Molecular-level insight into Cr/silica Phillips-type catalysts: polymerization-active mononuclear chromium sites", *J. Catal.* **205**, 366.

[4] Bordiga, S., Bertarione, S., Damin, A., Prestipino, C., Spoto, G., Lamberti, C. and Zecchina, A. (2003) "On the first stages of the ethylene polymerization on Cr^{2+}/SiO_2 Phillips catalyst: time and temperature resolved IR studies", *J. Mol. Catal. A: Chem.* **204–205**, 527.

[5] Liu, B. and Terano, M. (2001) "Investigation of the physico-chemical state and aggregation mechanism of surface Cr species on a Phillips CrO_x/SiO_2 catalyst by XPS and EPMA", *J. Mol. Catal. A: Chem.* **172**, 227.

[6] Liu, B., Nakatani, H. and Terano, M. (2002) "New aspects of the induction period of ethene polymerization using Phillips CrO_x/SiO_2 catalyst probed by XPS, TPD and EPMA", *J. Mol. Catal. A: Chem.* **184**, 387.

[7] Liu, B., Nakatani, H. and Terano, M. (2003) "Mechanistic implications of the unprecedented transformations of ethene into propene and butene over Phillips CrO_x/SiO_2 catalyst during induction period", *J. Mol. Catal. A: Chem.* **201**, 189.

[8] Pullukat, T.J. and Hoff, R.E. (1999) "Silica-based Ziegler-Natta catalysts: a patent review", *Catal. Rev.: Sci. Eng.* **41**, 389.

[9] McDaniel, M. (1985) "Supported chromium catalysts for ethylene polymerization", *Adv. Catal.* **33**, 47.

[10] Weckhuysen, B.M. and Schoonheydt, R.A. (1999) "Olefin polymerization over supported chromium oxide catalysts", *Catal. Today* **51**, 215.

[11] Limberg, C., Köppe, R. and Schnöckel, H. (1998) "Matrix isolation and characterization of a reactive intermediate in olefin oxidation with chromyl chloride", *Angew. Chem. Int. Ed.* **37**, 496.

[12] Boero, M., Parrinello, M. and Terakura, K. (1998) "First principles molecular dynamics study of Ziegler-Natta heterogeneous catalysis", *J. Am. Chem. Soc.* **120**, 2746.

[13] Seth, M. and Ziegler, T. (2003) "Polymerization properties of a heterogeneous Ziegler-Natta catalyst modified by a base: a theoretical study", *Macromolecules* **36**, 6613.

[14] Fujimoto, H., Yamasaki, T., Mizutani, H. and Koga, N. (1985) "A theoretical study of olefin insertion into Ti—C and Ti—H bonds. An analysis by paired interacting orbitals", *J. Am. Chem. Soc.* **107**, 6157.

[15] Kuribayashi, H.K., Koga, N. and Morokuma, K. (1992) "An *ab initio* MO study on ethylene and propylene insertion into the Ti—CH3 bond in Ch3TiCl2+ as a model of homogeneous olefin polymerization", *J. Am. Chem. Soc.* **114**, 2359.

[16] Fujimoto, H., Koga, N. and Hataue, I. (1984) “Orbital transformation in configuration analysis. A simplification in the description of charge transfer”, *J. Phys. Chem.* **88**, 3539.

[17] Fukui, K., Yonezawa, T. and Shingu, H. (1952) “A molecular orbital theory of reactivity in aromatic hydrocarbons”, *J. Chem. Phys.* **20**, 722.

[18] Shiga, A. (1999) “Theoretical study of ethylene polymerization on Ziegler-Natta catalysts and on metallocene catalysts”, *J. Mol. Catal. A: Chem.* **146**, 325.

[19] Shiga, A., Kawamura, H., Ebara, T., Sasaki, T. and Kikuzono, Y. (1989) “A theoretical study of the insertion of olefins into Ti-methyl bonds by ‘Paired Interacting Orbitals’”, *J. Organomet. Chem.* **366**, 95.

[20] Fujimoto, H. (1987) “Paired interacting orbitals: a way of looking at chemical interaction”, *Acc. Chem. Res.* **20**, 448.

[21] Johnson, J.R.T. and Panas, I. (2000) “Water adsorption and hydrolysis on molecular transition metal oxides and oxyhydroxides”, *Inorg. Chem.* **39**, 3181.